Advances in Colloid and Interface Science 256 (2018) 152–162

Contents lists available at ScienceDirect

Advances in Colloid and Interface Science

journal homepage: www.elsevier.com/locate/cis

Historical perspective

Zeta potentials of the rare earth element fluorcarbonate minerals focusing on bastnäsite and parisite

C.L. Owens [a,b,*], G.R. Nash [a], K. Hadler [c], R.S. Fitzpatrick [b], C.G. Anderson [d], F. Wall [b]

[a] College of Engineering, Mathematics and Physical Sciences, University of Exeter, Exeter EX4 4QF, United Kingdom
[b] Camborne School of Mines, University of Exeter, Penryn TR10 9FE, United Kingdom
[c] Department of Earth Science and Engineering, Imperial College London, SW7 2AZ London, United Kingdom
[d] Kroll Institute for Extractive Metallurgy, George S. Ansell Department of Metallurgical and Materials Engineering, Colorado School of Mines, Golden, CO 80401, United States

ARTICLE INFO

Available online 20 April 2018

Keywords:
Zeta potential
Fluorcarbonate minerals
Rare earth elements
bastnäsite
Parisite
Electrokinetics

ABSTRACT

Rare earth elements (REE) are critical to a wide range of technologies ranging from mobile phones to wind turbines. Processing and extraction of REE minerals from ore bodies is, however, both challenging and relatively poorly understood, as the majority of deposits contain only limited enrichment of REEs. An improved understanding of the surface properties of the minerals is important in informing and optimising their processing, in particular for separation by froth flotation. The measurement of zeta potential can be used to extract information regarding the electrical double layer, and hence surface properties of these minerals.

There are over 34 REE fluorcarbonate minerals currently identified, however bastnäsite, synchysite and parisite are of most economic importance. Bastnäsite–(Ce), the most common REE fluorcarbonate, supplies over 50% of the world's REE. Previous studies of bastnäsite have showed a wide range of surface behaviour, with the iso-electric point (IEP), being measured between pH values of 4.6 and 9.3. In contrast, no values of IEP have been reported for parisite or synchysite.

In this work, we review previous studies of the zeta potentials of bastnäsite to investigate the effects of different methodologies and sample preparation. In addition, measurements of zeta potentials of parisite under water, collector and supernatant conditions were conducted, the first to be reported. These results showed an iso-electric point for parisite of 5.6 under water, with a shift to a more negative zeta potential with both collector (hydroxamic and fatty acids) and supernatant conditions. The IEP with collectors and supernatant was <3.5. As zeta potential measurements in the presence of reagents and supernatants are the most rigorous way of determining the efficiency of a flotation reagent, the agreement between parisite zeta potentials obtained here and previous work on bastnäsite suggests that parisite may be processed using similar reagent schemes to bastnäsite. This is important for future processing of REE deposits, comprising of more complex REE mineralogy.

Contents

* Corresponding author at: College of Engineering, Mathematics and Physical Sciences, University of Exeter, Exeter EX4 4QF, United Kingdom.
E-mail address: co308@exeter.ac.uk (C.L. Owens).

https://doi.org/10.1016/j.cis.2018.04.009

1. Introduction

1.1. Rare earth elements (REE)

Rare earth elements (REE), which consist of the lanthanide (=lanthanoid) series of elements plus scandium and yttrium, as designated by the International Union of Pure and Applied Chemistry (IUPAC), and are used in a wide range of products in the engineering, space and energy sectors [1,2]. REE are often utilised in magnets due to their high remanence and coercivity, which is a result of the relatively large number of unpaired electrons in their atomic structure, in particular neodymium is a constituent of neodymium iron boron magnets [3]. Rare earth elements are contained within over 200 minerals and ore deposits located over seven continents [4–7], although the concentrations of REE within the ores are low and such they are difficult to process [2]. Although there is a broad range of interest in rare earth bearing minerals, with the European Commission identifying them as one of the twenty seven critical raw materials, the processing of them is still relatively poorly understood [8–10].

1.2. REE fluorcarbonates

REE fluorcarbonates are minerals which, consist of, but are not limited to, REE, F and CO_3 ions, most commonly in the general form REE (CO_3) F. Substitutions of elements such as thorium, sodium, barium and calcium into the lattice are rare, but in geological settings like Mont Saint Hilaire, exceptional minerals are formed such as horváthite ($NaY(CO_3)F_2$) and lukechangite ($Na_3\ Ce_2\ (CO_3)\ F$) [11,12]. REE are primarily sourced through the fluorcarbonate mineral bastnäsite-(Ce), sometimes spelled bastnaesite, which is the main ore mineral at the REE mine, Bayan Obo, China. Historically it was also mined in the Mountain Pass deposit, California, USA. Bastnäsite-(Ce) is also the most common mineral within the REE fluorcarbonate set of minerals and a member of the bastnäsite group which contains seven minerals (bastnäsite–(Ce), bastnäsite–(La), bastnäsite–(Nd), bastnäsite-(Y), hydroxylbastnäsite-(Nd), hydroxylbastnäsite-(Ce) and thorbastnäsite). Others minerals that are often linked to bastnäsite are parisite, synchysite and röntgenite (Table 1.2.1). First discovered in the Bastnäs mine in Sweden, after which it was named, bastnäsite has since been found in localities ranging from Pikes Peak Colorado to the moon [13–15]. In comparison, röntgenite was discovered in 1953 by Donnay and is very rare [16–19]. The nomenclature of rare earth fluorcarbonates requires that the dominant REE when specific to denoting a species is within parenthesis [20]. Table 1.2.1 shows the bastnäsite group of minerals plus parisite, röntgenite and synchysite.

REE fluorcarbonates can be differentiated by X-ray diffraction (XRD) which highlights differences in the crystal lattice and calcium content. Bastnäsite is calcium depleted, whereas synchysite contains over 16% calcium. Parisite and röntgenite form middle members of the series with 11% and 13% Ca content respectively.

Röntgenite and parisite are formed of layers along the c crystalline axis, the composition of which can be subdivided into bastnäsite (B) and synchysite (S) layers [17,18,43]. For a detailed insight into the structural and atomic arrangement of these minerals, this review suggests Ni et al. [19]. A summary of the composition is shown in Fig. 1.

REE fluorcarbonate minerals often exhibit irregularities in crystal structure such as syntaxial intergrowth and stacking faults [15,29]. This leads to irregularities in their chemical structure, which can cause challenges in isolating individual species using techniques such as XRF (X-ray fluorescence) and XRD. Al Ali [44] described a mineral altering

Table 1.2.1
Table of selected REE fluorcarbonates, chemical composition and examples of localities. Location lists the deposit name, country as stated by the literature, which may not cover modern borders. Chemical formulae are taken from International Mineral Association (IMA) Commission on New Minerals, Nomenclature and Classification (CNMNC). *Parisite-(Nd) not officially recognised by IMA CNMNC list as of July 2017.

Mineral	Example of locations	Chemical formula	Theoretical or measured chemical composition in oxides	Crystal system	Ref.
Bastnäsite-(Ce)	Bayan Obo, China. Mountain Pass, USA. Fen, Norway	$Ce(CO_3)F$	Ce = 63%. C = 5%. O = 21.9%. F = 8.67%	Hexagonal	[21,22]
Bastnäsite-(La)	Pike Peaks, Colorado, USA	$La(CO_3)F$	La = 63%. C = 5%. O = 22%. F = 8.72%	–	[15]
Bastnäsite-(Nd)	Clara Mine, Germany Stetind pegmatite, Norway	$Nd(CO_3)F$	Nd = 26%, La = 18%, Ce = 18%, F = 9%, (CO_2 was not measured due to paucity of mineral.)	Hexagonal	[23,24]
Bastnäsite-(Y)	Bayan Obo, China. Nissi Bauxite Laterite Deposit, Greece	$Y(CO_3)F$	Y = 52%. C = 7.15%. O = 28%.F = 11%	–	[25,26]
Thorbastnäsite	Yaja granite, China Eastern Siberia, Russia	$ThCa(CO_3)_2F_2\ 3H_2O$	Ce = 6.88%, C = 4.72%, Ca = 5.9%, Th = 45.57%, H = 1.19%, F = 7.46%	Hexagonal	[27,28]
Hydroxylbastnäsite-(Ce)	Kami-houri, Miyazaki Prefecture, Japan, Trimouns, France	$Ce\ (CO_3)(OH)$	Ce = 64%, O = 29%, C = 5.53%, H = 0.46%	Hexagonal	[29,30]
Hydroxylbastnäsite-(Nd)	Montenegro	$Nd\ (CO_3)\ (OH)$	Nd = 65%, O = 28%, C = 5.43%, H = 0.46%	Hexagonal	[31]
Parisite-(Ce)	Muzo, Bayaca, Columbia	$CaCe_2(CO_3)_3F_2$	Ce = 28%. La = 23%. C = 6%. O = 26%. F = 7%. Ca = 7%	Monoclinic	[32,33]
Parisite-(La)	Mula Mine, Bahia, Brazil	$CaLa_2(CO_3)_3F_2$		Monoclinic	[34,35]
*Parisite-(Nd)	Bayan Obo, China found in 1986	$CaNd_2(CO_3)_3F_2$	Nd = 23%. La = 20%. Ce = 10%. C = 6%. O = 25%. F = 6%. C = 6%	–	[36,37]
Röntgenite-(Ce)	Narssârssuk, Greenland (Denmark). Muso, Columbia	$Ca_2Ce_3\ (CO_3)_5F_3$	Ce = 37%. La = 12%. C = 7%.O = 28%. F = 6%. Ca = 9%.	Hexagonal	[16,17,19]
Synchysite-(Ce)	Songwe Hill, Malawi. Springer Lavergne, Canada	$CaCe(CO_3)_2F$	Ce = 43%. C = 8%. O = 30%. F = 6%. Ca = 13%	Monoclinic	[19,38,39]
Synchysite-(Y)	Kutessay, Kyrgyzstan	$CaY(CO_3)_2F$	Y = 33%. C = 9%. O = 36%. F = 7%. Ca = 14%.	Monoclinic	[40,41]
Synchysite-(Nd)	Triolet Glacier, Italy Grebnik deposit, Kosovo	$CaNd(CO_3)_2F$	Nd = 44%. C = 7%. O = 30%. F = 6%. Ca = 12%.	No XRD data	[41,42]

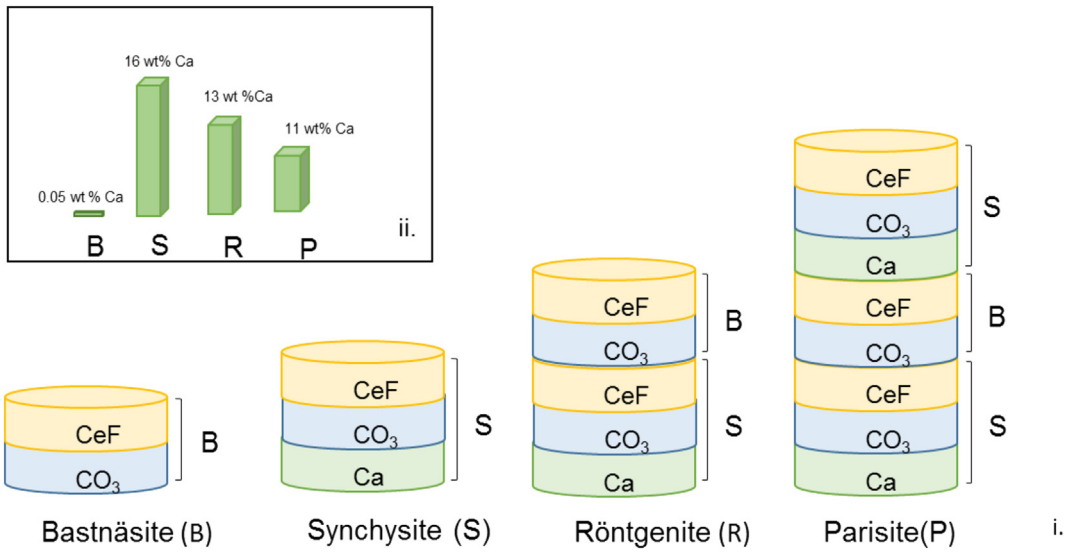

Fig. 1. i. Schematic of REE fluorcarbonate minerals showing the stacking along of the c-axis of the crystal. Röntgenite and parisite are made up of stacked layers of bastnäsite and synchysite (after Donnay and Donnay [17]; Van Landuyt and Amelincx [18]; Manfredi et al. [43]).ii. Calcium content of bastnäsite, synchysite, röntgenite and parisite minerals adapted from Al Ali [44].

from parisite to synchysite along its length using an electron microprobe. Syntaxial intergrowth can be seen in synchysite at sites such as Songwe Hill, Malawi, however the parisite and bastnäsite samples which were investigated in this review are not thought to exhibit syntaxial intergrowth or stacking irregularities [45]. The majority of the studies investigating bastnäsite focus on samples from Mountain Pass, which are not regularly affected by syntaxial intergrowth or other irregularities [10,45]. The purity of the samples and the corresponding effect on fundamental surface studies is covered later in this review.

1.3. REE mineral processing

REE minerals, in particular bastnäsite, are typically separated from the associated gangue minerals via froth flotation. Although REE deposits are sometimes processed additionally via other methods such as magnetic separation or gravity separation [10,46]. As REE deposits can contain a number of REE minerals, such as monazite, xenotime, and bastnäsite, multiple extraction methods are often combined to enable optimum separation [10,47] However, ion adsorption clays, which are another source of REE, are instead directly processed via hydrometallurgy techniques such as leaching [10].

Leaching if often conducted using sulfuric acid, which breaks down the crystal structure of the mineral [48]. As leaching using acids produces large amounts of toxic by-product new methods such as bioleaching of minerals with fungal and bacterial species such as *Aspergillus niger* and *Penicillium* sp. have recently been proposed [49,50]. Although bioleaching is an exciting area for further development current processing of REE minerals is still primarily conducted by froth flotation in China [10,51].

Froth flotation makes use of the differences in the surface properties between desired minerals and gangue; these differences can be optimised by altering the surface chemistry through the addition of chemical reagents. Flotation reagents for REE processing include collectors such as potassium lauryl phosphate, hydroxamic acids and fatty acids, which render the REE mineral particles hydrophobic, and depressants such as sodium carbonate, sodium silicate and lignin sulfonate, which act to increase the hydrophilicity and/or dispersion of the gangue minerals [10,52–57].There is a clear link between surface behaviour in the presence of flotation regents and mineral recovery, first demonstrated by Fuerstenau in 1957 [58]. Since then a large volume of flotation research has been dedicated to surface and colloidal science [59–61].

1.4. Surface behaviour

Surface behaviour describes a wide range of phenomena ranging from kinetic to electrochemistry, however as this review focuses on zeta potential measurements, the electrical double layer is described in detail. When a mineral is submerged in water the surface will acquire a charge due to a number of processes liberating ions including but not limited to preferential dissolution, hydration and surface group dissociation within the water, these free ions will form a counter layer or diffuse layer [62]. This charged area, the electrical double layer, can control the adsorption of collectors and reagents at the surface depending on the method of adsorption or attachment [63].The mineral surface properties determines which ions can bond with the electrical double layer [EDL], however all charged particles can form in the diffuse layer. The “potential determining ions” are the ions which affect the EDL and will either bond chemically with the surface, physisorb with the surface or link via Van der Waals force [63]. Physisorbed collectors are only effective when the mineral surface is oppositely charged to the collectors. Chemisorption, in comparison, can occur when the surface and the collector both carry the same charge, although if the Coulomb repulsion force is too large the collector will not be able to approach the surface to bond [59].

There have been many investigations into the mechanisms of fatty acid and hydroxamate adsorption onto REE minerals, using a range of methods from adsorption kinetic models to infrared spectroscopy [6,54,64,65]. Studies by Pavez et al. [64] and Jordens et al. [71] have shown chemisorption of hydroxamate and fatty acids, with both bonding with metal cations on the mineral surface [71].Other REE minerals such as monazite and ancylite have also been investigated showing they also chemisorb into hydroxamate [55,65].

1.5. The electrical double layer

The electrical double layer (EDL) describes the charged area between the mineral surface and the charged and counter charged ions attracted to that surface [63]. Although more recently this has been described as the electrical interfacial layer, due to its complex nature, the most common description has been the EDL and this nomenclature is

used in the remainder of the review. The most common method of characterizing the electrical double layer is by measuring the zeta potential [63]. Zeta potential is a measurement of the surface charge along the slip plane of the electrical double layer, and it can be probed using techniques such as electrophoresis, electro osmosis and streaming potential. In the majority of the work reviewed herein, the zeta potential was determined using either electrophoresis or streaming potential.

Both electrophoresis and streaming potentials as methods for measuring zeta potential contain limitations within the methodology [63]. For streaming potential the aqueous solution and mineral sample to be measured must be mechanically and chemically stable, for more soluble minerals this is problematic [63]. For electrophoresis measurements the concentration cannot be too high to allow particle mobility, as such different concentrations of reagents should be tested. For a full review of techniques for measuring zeta potential see Delgado et al. [63] Hunter [66] or Greenwood [67].

The most often quoted value for zeta potentials is the iso-electric point (IEP), when the zeta potential equals zero. This is of particular value in waste water treatment but is also utilised in many other fields such as mineral processing [48]. Zeta potentials are analysed over a wide range of pHs from alkaline to acidic to determine the IEP. Although the IEP and a second measure of zeta potential, point of zero charge (PZC), are often quoted as being the same thing, the PZC refers to the surface of the mineral having zero charge, whereas the IEP occurs when the zeta potential is zero [59]. For certain mineral surfaces under specific conditions IEP may equal PZC [59]. When reagents such as anionic or cationic collectors are adsorbed onto the mineral surface, a change in the IEP under constant reagent dosage is a measure of adsorption free energy [68].

Although zeta potential measurements are used to give indications of flotation they are often conducted in conjunction with micro-flotation or ultra-violet spectroscopy investigations to elucidate information on either floatability or adsorption of the mineral reagent system [53,65].

1.6. Zeta potential studies of REE fluorcarbonates

Bastnäsite is the only REE fluorcarbonate with published data for zeta potential measurements, with Smith and Steiner [69] reporting the first values of zeta potential over thirty years ago. The studies of the zeta potential of bastnäsite, which number twenty three at the time of writing, are summarised in Table 1.6.1. Although the review by Houot [70] has previously been referenced in papers as an investigation into bastnäsite, we do not reference it here as the paper consolidates previous results. Many of these previous investigations link zeta potential to micro-flotation experiments and the adsorption of various reagents at the surface [71,72], however comparisons of different studies is made difficult by the use of different methodologies, equipment and differing sample size, selection and preparation [62,63]. Kosmulski [73] showed that reviews of IEP and PZC often select results whose experimental method has not been described sufficiently well for clear comparison. The common practice to cite older works, and to ignore newer research, is also highlighted in that the work of Parks [74] is the most often cited for reviews of metal oxide PZC/IEP [73,74]. This paper, therefore, reviews the methodology, equipment and samples used to produce IEP measurements for REE fluorcarbonates so that future studies can make comparisons with ease.

In previous studies there is inconsistency in notation between PZC and IEP, with some authors referencing the point of zero charge of bastnäsite, whereas others reference the iso-electric point [71,75,76]. Table 1.6.1 denotes how the authors of each paper reference what they have done rather than how their work has later been referenced.

In most studies multiple samples of bastnäsite are not investigated, however Jordens et al. [71], showed that sample origin had a lesser effect on the measured IEP than methodology, with the electroacoustic methodology giving a much higher pH value for the same sample of bastnäsite at pH 8.1 than electrophoresis at pH 6.3. Although this review does not investigate this aspect further, it may be of future interest. Both samples were of bastnäsite-(Ce) so a hypothesis on the effect on the species of bastnäsite used is not possible at this time.

Table 1.6.1 shows that the majority of studies have been conducted on bastnäsite originating from Mountain Pass, California. This is not entirely unexpected due to the long period of extraction of the deposit located there, which was previously the prime source of REE from the 1980s [81]. The second most common locale for bastnäsite was Bayan Obo in China [87,88,90]. Bayan Obo currently supplies over 45% of the world REE and it is likely that more research has been conducted on bastnäsite from Bayan Obo which has either not been published due to non-disclosure agreements, or not been translated into English. Although in some studies the type of bastnäsite used in zeta potential measurements is not stated, the majority state the species used was bastnäsite-(Ce).

The effect of background solution has previously been investigated by a number of authors, with the concentration and ions present affecting the magnitude and value of zeta potential [75,81]. For more details on this topic see the review by Fuerstenau and Pradip [59].

The two main background electrolytes used in the studies reviewed in Table 1.6.1 are KCl and KNO_3. Potassium, chorine and nitrogen ions are not described as potential determining ions for bastnäsite and should not affect the IEP [84]. Although the majority of studies reviewed in Table 1.6.1 used KCl and KNO_3 as background electrolytes the concentration varied between studies, ranging from 10^{-1} M to 10^{-3} M. Notably, the three studies that used 10^{-1} M KNO_3 [72,76,79] had an IEP value of 7. However as these studies were conducted on the same ore (all contained some barite contamination), the effect of different parameters cannot be determined. Other studies state pure water as the background electrolyte. Pradip et al. [75] previously investigated the effect of using different background ions on zeta potential measurements of bastnäsite and found 10^{-3} M of $NaCO_3$ shifts to a lower IEP by one pH value. As sodium carbonate is often used in flotation systems as a depressant, this effect is expected. The differences in electrolyte type and concentration make comparison between the data difficult. Furthermore, Table 1.6.1 does not show that many of the studies also used different solutions to change the pH of the solution, thereby affecting ion concentration independently.

The purity of samples used is also difficult to determine, with some authors stating that the sample is handpicked (under UV light bastnäsite should glow green) and some stating % purity by conventional methods such as XRF or QEMSCAN [75,81]. XRD data is often additionally shown to compare to XRD data from a type locality such as hosted on the RRUFF database, which allows the identification of minerals via XRD by supplying a database of spectral analysis of minerals from different localities, for more details see Lafuente et al. [93]. The particle size is also variable, with some authors grinding the sample to <5 μm, but others using particle sizes over 75 μm. This disparity is assumed to be due to equipment and methodology.

The majority of studies used electrophoresis to measure the zeta potential by applying the Helmholtz-Smoluchowski equation. One study used the electroacoustic technique [71], the other studies listed in Table 1.6.1 did not specify which method was used.

Fig. 2 shows schematically the reported values of IEP and PZC of bastnäsite. The IEP of bastnäsite has been measured between pH 4.6 (Smith and Shonnard [89]) and pH 9.3 (Herrera-Urbina et al. [84]) [84,89]. The PZC of bastnäsite ranges from pH 7.8 to pH 9.2, however as there are only three studies with published values of PZC, compared to nineteen values of IEP it is difficult to compare the two. There is no obvious historical bias of IEP, with Pradip et al. [75] recording a value of 5.3 in 2015, and Sarvaramini et al. [78] recording a year later an IEP of 9. There is also no discernible geological effect, with samples of bastnäsite from Mountain Pass with IEP values ranging from pH 4.7 to pH 9.3. The Mountain Pass ore body has shown large variation between bastnäsite compositions, with areas showing different enrichment or

Table 1.6.1
Published studies on the surface behaviour investigations into bastnäsite. Purity column uses the description of purity stated within the reference. Blanks within the column are due to the information not being stated within the referenced material. Gaps in the table correspond to where literature does not specify details. For results from Pradip (2015) the "also" between values of electrolytes denotes that the study conducted two experiments with different electrolytes.

Mineral	Deposit	Country	Purity	Size μm	PZC	IEP	Background Electrolyte	IEP in collector	Method	Year	Study
Bastnäsite (Ce)	–	–		$D_{50} = 2.3$		7–8	10^{-3} M/L NaCl		Electrokinetic	2017	Espiritu et al., 2017 [77]
Bastnäsite	Mountain Pass	USA	Some barite	<5	–	7	10^{-1} M KNO_3	na	–	2017	Azizi et al., 2017 [72]
Bastnäsite (Ce)	Mountain Pass	USA	Some barite	<5	–	7	10^{-1} M KNO_3	5.8		2016	Sarvaramini et al., 2016 [78]
Bastnäsite	–	–	–	<10	–	8	10^{-3} M NaCl		–	2016	Espiritu et al., 2016 [79]
Bastnäsite	Zagi Mountain	Pakistan		−45		9	–		–	2016	Liu et al., 2016 [80]
Bastnäsite	Mountain Pass	USA	Some barite	<5	–	7	10^{-1} M KNO_3	4	–	2016	Azizi et al., 2016 [76]
Bastnäsite-(Ce)	–	–	Handpicked	<32	–	8.2	–	6.6, 5.2		2015	Anderson 2015 [81]
Bastnäsite-(Ce)	Mountain Pass	USA	57.4 REO% compared to 75 pure REO%	<37	9.2	–	10^{-3} M $NaNO_2$ Also 10^{-3} M NaF		–	2015	Pradip et al., 2015 [75]
Bastnäsite	Synthetic	–	100% pure		7.8		10^{-3} M $NaNO_2$ Also 10^{-3} M NaF			2015	Pradip et al., 2015 [75]
Bastnäsite	Zagi Mountain	Pakistan		−45	8.1				Micro-electrophoresis	2014	Zhang 2014 [82]
Bastnäsite	–	–	72.05REO %	−25	–	5.3	10^{-2} M KCl	–	–	2014	Fang et al., 2014 [83]
Bastnäsite-(Ce)	Mountain Pass	USA		d50 = 1.9	–	6.4	10^{-3} M KCl	8.9	Electrophoresis	2014	Jordens et al., 2014 [71]
Bastnäsite-(Ce)	–	Madagascar		d50 = 2	–	8.1	10^{-3} M KCl	10.2	Electroacoustic	2014	Jordens et al., 2014 [71]
Bastnäsite-(Ce)	–	Madagascar		d50 = 2	–	6.2	10^{-3} M KCl	7.6	Electrophoresis	2014	Jordens et al., 2014 [71]
Bastnäsite	Birthday Claim, Mountain Pass	USA	52% cerium	75	–	9.3	Na NO_3	–	Electro kinetic	2013	Herrera-Urbina et al., 2013 [84]
Bastnäsite-(Ce) or Bastnäsite-(La)	Zagi Mountain	Pakistan	–	45	8.1		–	–		2013	Zhang et al., 2013 [85]
Bastnäsite		Vietnam				4.7	–			2010	Kim et al., 2010 [86]
Bastnäsite	Haoniuping Mine	China	96.50% pure	37	–	7.8	–	–	Electrophoresis	2000	Ren et al., 2000 [87]
Bastnäsite-(Ce)	Maoniuping Mine, Sichuan Province	China	98.10% pure	37	–	8	Water	5.9	Electrophoresis	1997	Ren et al., 1997 [88]
Bastnäsite-(Ce)	Pocos de Caldas, MG.	Brazil	–	37	–	4.9	10^{-3} KCl	4.2	Micro-electrophoresis	1996	Pavez et al., 1996 [64]
Bastnäsite	Mountain Pass	USA	Handpicked	<10	–	4.6	Pure water	–	–	1986	Smith and Shonnard 1986 [89]
Bastnäsite	Bayan Obo	China	Handpicked	10	–	7	10^{-3} KNO_3	–	Electrophoresis	1984	Luo and Chen 1987 [90]
Bastnäsite	Synthetic		100%			7.8	Pure water			1982	Li 1982 [91]
Bastnäsite	Mountain Pass	USA				9.25	–			1981	Pradip 1981 [92]
Bastnäsite	Mountain Pass	USA	Handpicked	1–10	–	5.3 (>30 min)	water-		Electrophoresis	1980	Smith and Steiner 1980 [69]
Bastnäsite	Mountain Pass	USA	Handpicked	1–10		6.8 (2 h)	water-		Electrophoresis	1980	Smith and Steiner 1980 [69]
Bastnäsite	Mountain Pass	USA	Handpicked	1–10		7.2 (24 h)	-water		Electrophoresis	1980	Smith and Steiner 1980 [69]

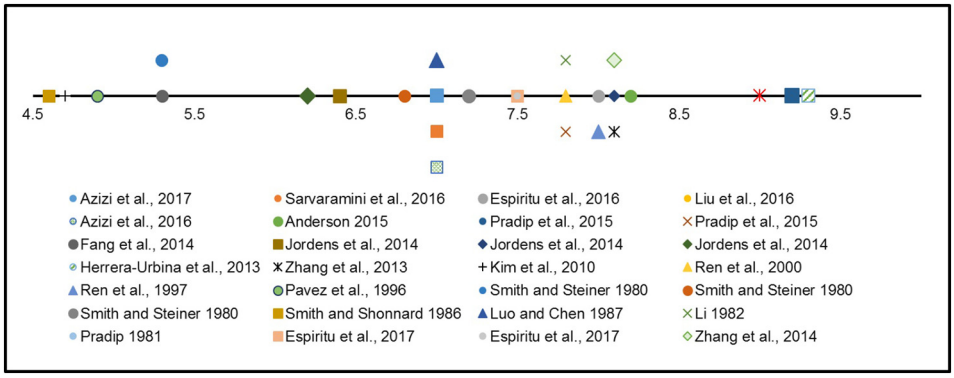

Fig. 2. The IEP and PZC of previous studies into bastnäsite. After Jordens et al. [71]. Bastnäsite from Mountain Pass is shows as a square. Bastnäsite from China is marked as a triangle. Bastnäsite from unknown deposit is marked as a circle. Diamond is from Madagascar. Star is from Pakistan and the cross is synthetic bastnäsite.

REE within the bastnäsite, this variation may explain the large range in values of IEP from minerals from the same body. Synthetic bastnäsite has been found to have an IEP at pH 7.8, however both studies on synthetic bastnäsite were conducted by the same authors [75,91]. Synthesis of the bastnäsite followed the same methodology, with Li [91] using a Zetameter whereas Pradip et al. [75] used a Riddick Zetameter (Model 3). It is unknown whether the same results would be obtained from synthetic bastnäsites using different methodologies for production or in different laboratories. Bastnäsite from Zagi Mountain has produced IEP values between pH 9 and pH 8.3, with the only PZC value at pH 8.1, a smaller range than samples from Mountain Pass [80,82,85].

From the results summarised in Table 1.6.1, it is difficult to determine a clear trend or value set that would allow a bastnäsite sample or a sample that behaves like bastnäsite to be clearly differentiated using IEP or PZC. The review by Kosmulski [62] found similar challenges when comparing the IEP and the PZC of materials other than metal oxides, however there was less variation in IEP compared to PZC. This was attributed to the selection of only electrokinetic studies for IEP values. The same methodology cannot be applied here due to the scarcity of studies which specify the methodology. There are also too few studies to allow any statistical analysis of parameters such as particle size or methodology.

In the review, we have consolidated previous studies of bastnäsite zeta potential for future research. We have also investigated the surface behaviour of the other REE fluorcarbonates, specifically parisite. Parisite is important as a possible accessory REE ore mineral in a range of deposits including Kamthai deposit, India and Khanneshin, Afghanistan [94,95]. Although bastnäsite has been intensively researched for the last 30 years, no fundamental studies have been published on any other REE fluorcarbonates. In this study, we therefore report the first values of the zeta potential of parisite measured using streaming potential under water, collector and supernatant conditions. This is consistent with previous studies conducted on bastnäsite [71,79]. Surface behaviour research into bastnäsite has been applied to the flotation of other REE fluorcarbonates, usually when they are not the principle ore mineral [96,97]. The aim of the experimental study in this work is to validate this approach by the comparison of zeta potential measurements of parisite and bastnäsite.

2. Materials and methods

2.1. Mineral and reagents

A mineral sample of parisite-(Ce) from Snow Bird Mine, Mineral Country, Montana, USA was acquired from Ikon Minerals. Parisite-(Ce) is the only REE fluorcarbonate mineral identified at the Snowbird Fluorite REE deposit. The sample used was large (approximately 10 cm long), and yellowish brown/brown in colour, consistent with parisite samples from this locality [98,99]. The sample purity was analysed using XRF (ARL PERFORM'X Sequential X-Ray Fluorescence Spectrometer, Thermo Fisher), at the Colorado School of Mines, and the elemental compositional analysis is shown in Table 2.1.1 (full results are given in the Supplementary material).

From XRF analysis, the parisite-(Ce) is fluorine depleted with high concentrations of the REEs, cerium, lanthanum and neodymium, and contains barium and silicon. These results are in agreement with previous analysis from Metz [100] who found significant concentrations of calcium, cerium, lanthanum, neodymium, praseodymium and yttrium in parisite–(Ce) from Snowbird.

Two types of collectors were acquired, a fatty acid supplied by Betachem (product name Betacol CKF 30B) and hydroxamic acid (product name AM810) supplied by Axis House, South Africa. These collectors were selected as hydroxamic and fatty acids are the most common collectors used in bastnäsite flotation, therefore zeta potential results from parisite can be compared to bastnäsite [10].

The supernatant from a mixed calcite/ankerite/synchysite/apatite ore was created by diluting the ore to 20% (wt) with DI water and heating to 60C for 30 min whilst agitating with a magnetic stirrer at 120 rpm. The solids were then separated via filtration. The supernatant was generated to approximate conditions in a flotation system of a mixed ore. Measurements using ICP-OES on an identical sample showed 11.97 mg/L of Ca ions, 1.5 mg/L Mg ions and 0.05 mg/L of Fe ions in the supernatant.

2.2. Zeta potential measurements

The parisite-(Ce) sample was a single mineral, virtually free from contamination and was first ground via steel ring mill (Angstrom Model TE250 Ring Pulverizer) to 100% passing 80 μm. Due to the paucity of the mineral sample, grinding curves to establish the time to reach the target particle size distribution were produced using proxy samples of

Table 2.1.1
XRF results from parisite sample showing oxide composition. wt% is stated for all values >2%. For a full list of elemental composition see Supplementary material.

Compound	Wt%
Y_2O_3	2.73
La_2O_3	16.99
$Ce\ O_2$	33.62
Pr_6O_{11}	3.67
$Nd_2\ O_3$	13.09
Sm_2O_3	1.81
Gd_2O_3	1.57
CaO	13.46
ThO_2	2.75
BaO	2.67
$Si\ O_2$	2.23

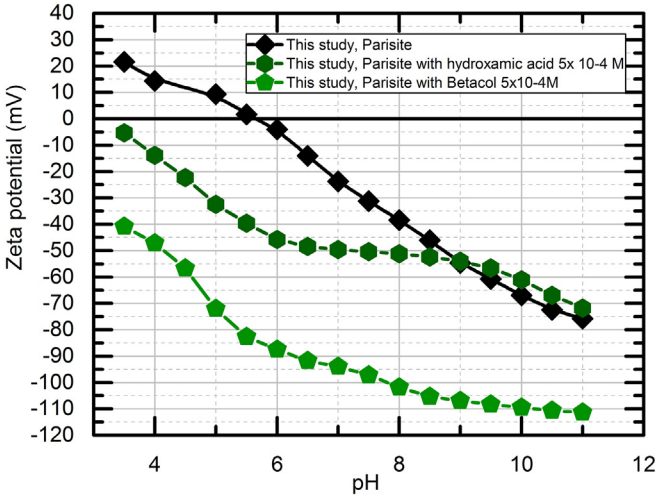

Fig. 3. Zeta potential of parisite in DI under the hydroxamate collector of 5×10^{-4} mol/L and under 5×10^{-4} mol/L of betacol fatty acid collector.

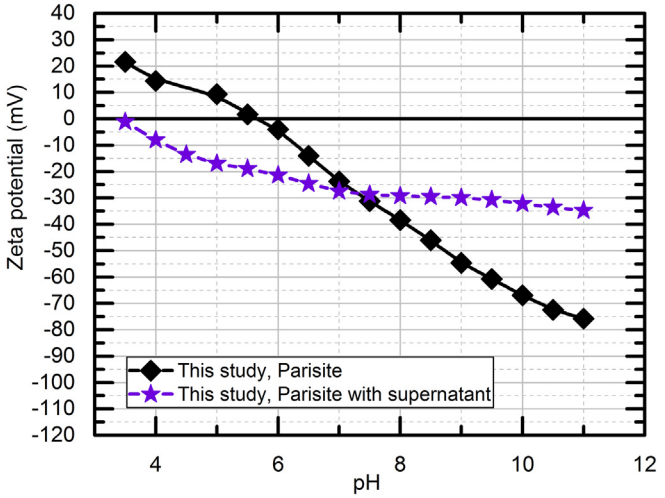

Fig. 4. Zeta potential of parisite under DI and parisite under supernatant conditions.

calcite [101]. More details of calcite and REE fluorcarbonate properties can be found in Miyawaki et al. [102] and Pavese et al. [103]. The mineral samples were suspended in water or collector solution at 0.02 g per 40 mL and then agitated on a shaking table for 20 min before each measurement. Surface behaviour measurements were conducted using the Microtrac Stabino Particle Charge Mapping surface chemistry device at Colorado School of Mines, U.S.A.

3. Results

The surface charge of parisite was measured as a function of pH, between pH 3.5 and pH 11, the results are shown in Fig. 3. The iso-electric point for parisite-(Ce) was measured at a pH of 5.6 in water. The charge of parisite decreases linearly as pH increases above 6, suggesting an uptake of negatively charged species at the surface (or the loss of positively charged species at the surface). Although most surfaces are positively charged at acidic pH and negatively charged at base pH [62], the magnitude and gradient of the zeta potential results agrees with those of bastnäsite [71,81].The sign and magnitude of the charge indicate the uptake of different species in the solution. In semi-soluble salts such as bastnäsite [101] the main species of potential determining ions that are at the surface have been found to be CeF, $CeFCO_3$, $Ce(OH)_3$, CeF_3 [84], as shown in Table 3.1. As parisite and bastnäsite have largely the same composition, apart from a higher Ca content in the parisite, it is reasonable to assume that the surface ions are controlled by some of the same species, however a full investigation of this is beyond the scope of this paper.

3.1. Behaviour under collector conditions

Both hydroxamic acid and betacol (fatty acid) are anionic collectors and as such it can be expected that they would reduce the surface charge of the mineral surface. In Fig. 3, the zeta potential (mV) is plotted against the pH of parisite under water, hydroxamate (5×10^{-4} mol/L) and fatty acid (5×10^{-4} mol/L) conditions. Both hydroxamate and fatty acids reduce the surface charge so the IEP < 3.5, with the surfaces negatively charged between pH 3.5 and pH 11. This is a shift of the IEP by a minimum of 2.1 from the IEP of parisite in water of 5.6. The hydroxamic acid affects the parisite surface to a lesser degree than the fatty acid, reducing the surface charge at pH 3.5 to −5.3 mV compared to −40.9 mV for betacol. Between pH 9 and pH 11 the zeta potential of parisite in hydroxamic acid is more positive than parisite in water. Zeta potential measurements by Sarvaramini et al. [78], on bastnäsite treated by hydroxamic collector found a similar trend between pH 9 and pH 11 with investigations by FTIR showing less negatively charged heptyl hydroxamic acid anions attached to the surface between these pH values.

Table 3.1
Ions affecting surface behaviour of bastnäsite zeta potentials over different pH ranges.
Taken from Jordens et al. [71] adapted from Herrera-Urbina et al. [84].

pH range	Ions
<5.2	CeF
5.22–5.74	$CeFCO_3$, CeF_3
5.74–8.55	$CeFCO_3$
8.56–10.12	$CeFCO_3$, $Ce(OH)_3$
>10.2	$Ce(OH)_3$

3.2. Behaviour under supernatant conditions

Fig. 4 shows that the zeta potential of parisite at pH 3.5 changed from 21.6 mV in water to −1.1 mV with supernatant background. In supernatant background, the zeta potential decreases by 10.2 mV, between pH 7 and pH 11, whilst between pH 7 and pH 3, the value changes by 38.9 mV, suggesting a greater effect at lower pH values. Between pH 7 and pH 11 the zeta potential of parisite in supernatant was higher than parisite in water. Espiritu et al. [79], who conducted zeta potential measurements of bastnäsite in dolomite supernatant, between pH 8.2 and pH 10 the zeta potential of bastnäsite under supernatant was more positive than bastnäsite in water. Previous work by Pradip et al. [104] and Espiritu et al. [79] linked the lowered surface charge under supernatant conditions of a carbonatite to adsorption of carbonate ions at the surface of the mineral [79,104].

4. Discussion

The zeta potential measurements obtained for parisite can be compared to previous research conducted on bastnäsite (Table 1.6.1). The IEP of the parisite sample recorded was 5.6; this lies towards the lower end of previous IEP values obtained for bastnäsite, which ranged from pH 4.7 to pH 9.3 (Fig. 2). The methodology used in selecting the specimen of parisite was handpicked, with the XRF checking the purity of the sample afterwards, this follows methodology used by Anderson [81]. The size of the mineral sample at 100% passing 80 μm was also larger than the majority of other studies reviewed in Table 1.6.1, however a direct comparison of grind size is difficult due to the differences

in sample analysis. The background for measurements was water, the same as for bastnäsite samples by Ren et al. [88].

Of the twenty one previous studies of bastnäsite, fifteen were identified as having extractable zeta potential values. Of these fifteen, five were selected due to their specification of purity of the sample of bastnäsite used in the study [71,83,87,88]. It must be noted that the samples had both different source localities and that they were measured under different electrolytes. The results of Anderson [81] were additionally selected due to the use of the same experimental equipment and methodology. These are compared to the results obtained for parisite in Fig. 5, where, for each study, six values of zeta potential at pH values around 3, 5, 6, 7, 9, 11 were extracted.

As can be seen in Fig. 5, the zeta potential measurements for bastnäsite and parisite share many similarities. The IEP of parisite obtained lies between the values of the selected studies of pH 5.3 (Fang et al. [83]) and pH 8.2 (Anderson [81]). The value of zeta potential at pH 3.5 of four of the six studies was between 20 and 35 mV which is within the range of the parisite value of 21 mV. The results at more alkaline pH differ to a greater degree, with parisite having a zeta potential of −76 mV at pH 11.5; although this value is much greater than the nearest bastnäsite selected for this comparison, (−40 mV from Anderson [81]), Pavez et al. [64] recorded a surface charge of −70 mV at pH 11.5 for the sample of bastnäsite from Brazil [64]. If directly compared to bastnäsite from the study by Anderson [81], the IEP for parisite is lower than bastnäsite.

While absolute values of zeta potential are of interest, it is the response to different surfactants that is of particular importance for REE processing. Values from literature suggest that under collector (hydroxamate) conditions, parisite also behaves similarly to bastnäsite. The shift of the parisite IEP to a lower value under hydroxamate conditioning agrees with the majority of previous investigations, excluding Jordens et al. [71]. Anderson [81] recorded a shift to an IEP of 6.6 (10^{-4} M of hydroxamic acid) and 5.2 (with 10^{-3} M of hydroxamic acid) under hydroxamate conditions. Saravaramini et al. [78] and Azizi et al. [72] both conducted zeta potential measurements with samples conditioned in Aero brand collector hydroxamates, this moved the IEP of bastnäsite from 7 to 5.8 and 7 to 4 respectively. This agreed with earlier work by Ren et al. [87], and Pavez et al. [64]. In comparison, Jordens et al. [71] found a shift to a higher IEP value of 8.9 with the bastnäsite from Mountain Pass, and a pH of 7.6 with the bastnäsite from Madagascar. This was attributed to the use of a different type of hydroxamic acid, a benzohydroxamic acid instead of octyl hydroxamic acid. Jordens et al. [71] suggesting that the increase in surface charge may have been due to the adsorption of REE metal hydroxamate complexes onto the mineral surface.

Two studies were selected to compare the effect of hydroxamic acid on bastnäsite and parisite (Ren et al. [88] and Anderson [81]), shown in Fig. 6. These two studies were selected as Ren et al. [88] used a highly pure bastnäsite sample, whereas Anderson [81] used the same methodology and equipment used for parisite in our investigation. In both studies, the IEP of bastnäsite shifted to a lower value under hydroxamate reagent addition. As can be seen in Fig. 6, the hydroxamate lowers the zeta potential of the bastnäsite across the entire pH range investigated by all studies, as it does for the parisite investigated in this study. In Ren et al. [88] the hydroxamate (named MOHA) was proven to chemisorb onto the mineral surface with maximum adsorption occurring at pH 8–10, with the hydroxamate shown to chelate with the cerium ions at the surface of bastnäsite. Anderson [81] showed adsorption was also chemical in nature with greater adsorption at elevated temperatures. The similarities in the observed behaviour of bastnäsite and parisite, as seen in Figs. 5 and 6, suggest that hydroxamate also chemisorbs onto parisite.

To compare the effect of the supernatant on parisite to the effect on bastnäsite, results from this research were compared to values from Espiritu et al. [79], with values of zeta potential plotted as a function of pH in Fig. 7. Analysis (using ICP-OES) of the supernatant used in our investigation indicated the presence of calcium ions, magnesium ions and iron ions in small quantities. In contrast to the behaviour under water conditions, the measured zeta potential of both bastnäsite and parisite has a weak dependence on the pH under supernatant conditions. The depression of the zeta potential to a set charge is in line with previous research by Al Marouqi et al. [105] which showed zeta potential does not change as a value of pH but as a function of pCa ions. Although work has been undertaken regarding the solubility of hydroxylbastnäsite by Voigt et al. [106], there have been no specific studies on the solubility of parisite, therefore differences between the two cannot be determined [106]. The effect of the supernatant is important for future processing of parisite and the other REE fluorcarbonates, as effects on the surface charge could affect or be an indicator of collector adsorption [77].

Collector adsorption under supernatant conditions has recently been explored by Espiritu et al. [77]. Bastnäsite surface behaviour under a dolomite supernatant was investigated and Ca^{2+} from the supernatant was found to possibly adsorb onto the bastnäsite via covalent bonds

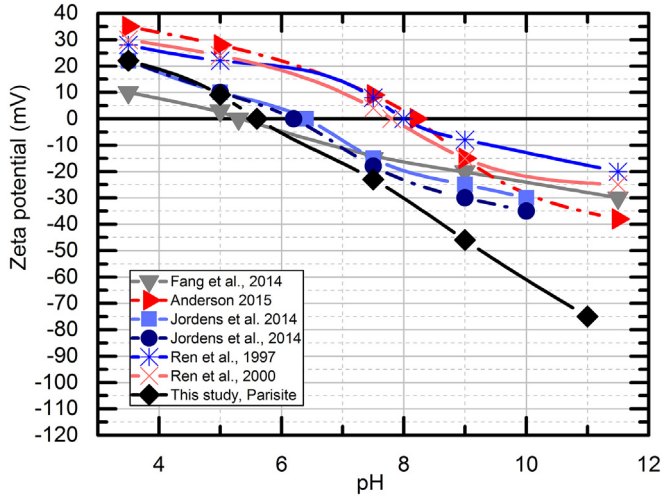

Fig. 5. Comparison of previous bastnäsite zeta potential studies with this studies zeta potentials (Ren et al. [87]; Ren et al. [88]; Fang et al. [83]; Jordens et al. [71]; Jordens et al. [71]; Anderson [81]). Values of zeta potential (mV) were taken from papers at pH 3.5, 5, 7.5, 9, 11.5 and the IEP values are accurate to within 5 mV. IEP are clearly reported in the papers and transferred on the plot. Six points were selected to show characteristic of the zeta potential value under different pH conditions.

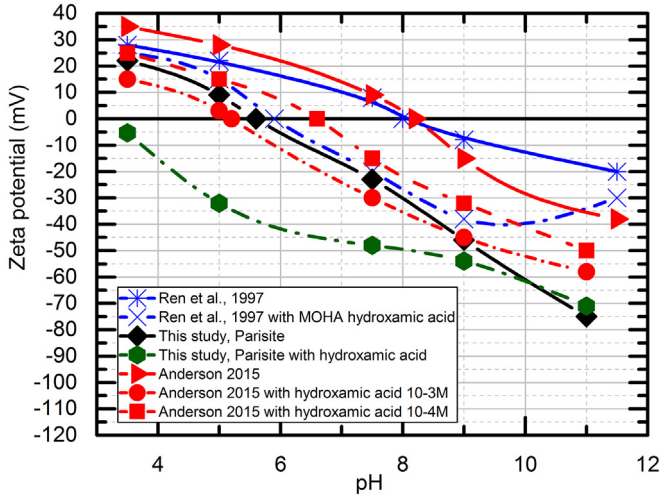

Fig. 6. Zeta potentials of bastnäsite under DI water conditions (Ren et al. [88], Anderson [81]), under hydroxamic acid MOHA conditions (Ren et al. [88] with MOHA) and under hydroxamic acid conditions (Anderson [81]). Zeta potentials of parisite, zeta potentials of parisite with hydroxamate at 5×10^{-4} M.

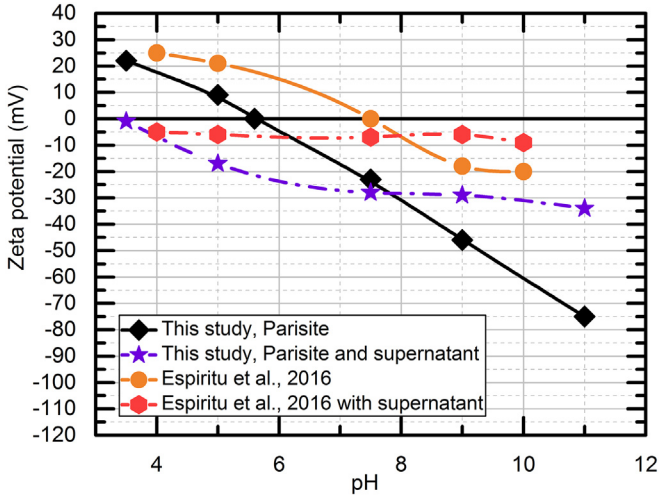

Fig. 7. Zeta potentials of extracted from published data from Espiritu [79] on the supernatant of dolomite and its effect on the zeta potential of bastnäsite. Zeta potentials of parisite and parisite under mixed calcite-ankerite supernatant.

limiting collector adsorption [77].Further research using XPS or FTIR into the interactions between collectors, supernatant and parisite would demonstrate the exact mechanism of adsorption or bonding.

As the main difference between parisite, bastnäsite, röntgenite and synchysite is small changes within the calcium content, and parisite and bastnäsite appear to have corresponding surface behaviour it is reasonable to expect this would extend to röntgenite and synchysite.

Although further work is required to investigate the application of these findings to mineral separations, if the surface behaviour of REE fluorcarbonates is the same across the series, then much of the research that has been conducted on bastnäsite deposits could be applied to synchysite, röntgenite and parisite deposits. Currently there are multiple deposits with REE fluorcarbonates under exploration such as Springer Lavergne, Quebec containing synchysite (Ce) and Mt. Prindle, AK, USA containing synchysite and parisite [32].

Applying bastnäsite surface behaviour, in particular the Mountain Pass and Bayan Obo deposit research, to other REE fluorcarbonate deposits already occurs, particularly when synchysite is not the principle ore mineral [107,108]. It is challenging to quantify how widespread this practice may be as it is rare to publish detail of the processing [109], however this review provides the first step towards scientific validation of this approach.

In exploration and development of REE deposits, not only is the deposit size vital but, particularly in the case of REE, the ease of extraction is extremely important. If it is possible to predict that all REE fluorcarbonates behave in a similar way to bastnäsite during flotation, then much of the research that has already been conducted into surface behaviour with regards to reagent addition remains valid.

5. Conclusion

In conclusion, zeta potentials measurements of parisite, the first of their kind produced an iso-electric point (IEP) of pH 5.6. This value is at the lower end of the IEP values of bastnäsite, which range from pH 4.6 to pH 9.3 in the literature. Under reagent collector conditions parisite behaves in a similar way to bastnäsite, with the value of zeta potential decreasing with increasing pH, and the IEP shifting to lower values compared to those obtained under water conditions. This similar behaviour extends to zeta potential values under supernatant conditions, where a decrease in zeta potential values was measured, compared to those obtained under water, as have previously been observed for bastnäsite. As many REE fluorcarbonate deposits, particularly those containing synchysite and parisite are already processed in a similar way to bastnäsite, this research validates this approach. This is important for future processing of REE deposits, comprising of more complex REE mineralogy.

Supplementary data to this article can be found online at https://doi.org/10.1016/j.cis.2018.04.009.

Acknowledgements

This research was conducted thanks to funding by the UK's Natural Environment Research Council SoS RARE Grant Agreement No. NE/M 011429/1 and Mkango Resources Ltd. Support was also provided by Kroll Institute for Extractive Metallurgy, Department of Metallurgy and Materials Engineering, Colorado School of Mines. Work could not have been conducted without collaboration between the Critical Materials Institute and the SoS RARE project. Special thanks to Hao Cui and Dylan Everly of Colorado School of Mines for support on the Microtrac Stabino equipment and XRF. Travel costs for visiting researcher collaboration provided by a Camborne School of Mines Travel Trust Grant. Special thanks to Tom Leistner and Edgar Schach at Helmholtz Institute Freiberg for Resource Technology for analysis of the supernatant via ICP-OES. C.L. Owens would also like to acknowledge Clara Montgomery for reading through the manuscript.

Data presented in the graphs relating to Parisite-(Ce) are publicly accessible through the British Geological Survey National Geoscience Data Centre [110].

Conflicts of interest

None.

References

[1] Hatch GP. Dynamics in the global market for rare earths. Elements 2012;8:341–6.
[2] Wall F. Rare earth elements. In: Gun G, editor. Critical metals handbook. Chichester, UK: John Wiley & Sons Ltd.; 2014. p. 312–39.
[3] Zhang S, Ding Y, Liu B, Chang CC. Supply and demand of some critical metals and present status of their recycling in WEEE. Waste Manag 2017;65:113–27.
[4] Goodenough KM, Wall F, Merriman D. Nat Resour Res (Dordrecht, Neth) 2017: 1–16.
[5] Tsubokawa Y, Ishikawa M, Kawakami T, Hokada T, Satish-Kumar M, Tsuchiya N, et al. Pressure–temperature–time path of a metapelite from Mefjell, Sør Rondane Mountains, East Antarctica. J Mineral Petrol Sci 2017;112(2):77–87.
[6] Abaka-Wood GB, Addai-Mensah J, Skinner W. A study of flotation characteristics of monazite, hematite, and quartz using anionic collectors. Int J Miner Process 2017; 158:55–62.
[7] Broom-Fendley S, Brady AE, Horstwood MS, Woolley A, Mtegha J, Wall F, et al. Geology, geochemistry and geochronology of the Songwe Hill carbonatite, Malawi. J African Earth Sci 2017;134:10–23.
[8] Wall F, Rollat A, Pell RS. Responsible sourcing of critical metals. Elements 2017;13 (5):313–8.
[9] Communication from the Commission to the European Parliament, The Council, The European Economic and Social Committee and the Committee of Regions on the 2017 list of Critical Raw Materials. Brussels, 13.9.2017.COM/2017/0490/final.
[10] Jordens A, Cheng YP, Waters KE. A review of the beneficiation of rare earth element bearing minerals. Miner Eng 2013;41:97–114.
[11] Grice JD, Chao GY. Horváthite-(Y), rare-earth-fluorocarbonate, a new mineral species from Mont Saint-Hilaire, Quebec. Can Mineral 1997;35:743–9.
[12] Grice JD, Chao GY. Lukechangite-(Ce), a new rare-earth-fluorocarbonate mineral from Mont Saint-Hilaire, Quebec. Am Mineral 1997;82(11–12):1255–60.
[13] Holtstam D, Andersson UB. The REE minerals of the Bastnäs-type deposits, South-Central Sweden. Can Mineral 2007;45:1073–114.
[14] Mokhov AV, Kartashov PM, Bogatikov OA, Ashikhmina NA, Magazina LO, Koporulina EV. Fluorite, hatchettolite, calcium sulfate, and bastnasite-(Ce) in the lunar regolith from Mare Crisium. Dokl Earth Sci 2008;422:1178–80.
[15] Müller MM, Kleebe HJ, Lauterbach S, Zito G. Crystallographic orientation relationship between bastnaesite, fluocerite and cerianite observed in a crystal from the pikes peak pegmatites. Z Kristallogr Cryst Mater 2011;226:467–75.
[16] Donnay G. Roentgenite, $3CeFCO_3 \cdot 2CaCO_3$, a new mineral from Greenland. Am Mineral 1953;38:868–70.
[17] Donnay G, Donnay JDH. The crystallography of bastnaesite, parisite, roentgenite, and synchysite. Am Mineral 1953;38:932–63.
[18] Van Landuyt J, Amelinckx S. Multiple beam direct lattice imaging of new mixed-layer compounds of the bastnäsite-synchysite series. Am Mineral 1975;60:351–8.

[19] Ni Y, Hughes JM, Mariano AN. The atomic arrangement of bastnäsite-(Ce), $Ce(CO_3)F$, and structural elements of synchysite-(Ce), röntgenite-(Ce), and parisite-(Ce). Am Mineral 1993;78:415–8.
[20] Bayliss P, Levinson AA. A system of nomenclature for rare-earth mineral species: revision and extension. Am Mineral 1988;73(3–4):422–3.
[21] Andersen T. Compositional variation of some rare earth minerals from the Fen complex (Telemark, SE Norway): implications for the mobility of rare earths in a carbonatite system. Mineral Mag 1986;50:503–9.
[22] Kanazawa Y, Kamitani M. Rare earth minerals and resources in the world. J Alloys Compd 2006;408:1339–43.
[23] Kolitsch U, Graf HW, Blaß G. Untersuchungen über die Seltenerden-Carbonate Bastnäsit und Synchisit von der Grube Clara im Schwarzwald: Nachweis von Bastnäsit-(Ce), Bastnäsit-(Nd), Bastnäsit-(La) und Synchisit-(Ce). Aufschluss 1997;48:367–79.
[24] Miyawaki R, Yokoyama K, Husdal T. Bastnäsite-(Nd). Mineral Mag 2011;75:2887–93.
[25] Yang XY, Sun WD, Zhang YX, Zheng YF. Geochemical constraints on the genesis of the Bayan Obo Fe–Nb–REE deposit in Inner Mongolia, China. Geochim Cosmochim Acta 2009;73:1417–35.
[26] Kalatha S, Perraki M, Economou-Eliopoulos M, Mitsis I. On the origin of bastnaesite-(La, Nd, Y) in the Nissi (Patitira) bauxite laterite deposit, Lokris, Greece. Minerals 2017;7:45.
[27] LiMin Z, ZengQian H, YuanChuan Z, Wei L. Study on accessory minerals in Yaja granite, northern Tibet: indicator of the magma source. Acta Petrol Sin 2011;27(9):2786–94.
[28] Fleischer M. New mineral names. Am Mineral 1965;50:1505.
[29] Michiba K, Miyawaki R, Minakawa T, Terada Y, Nakai I, Matsubara S. Crystal structure of hydroxylbastnäsite-(Ce) from Kamihouri, Miyazaki Prefecture, Japan. J Mineral Petrol Sci 2013;108(6):326–34.
[30] Yang H, Dembowski RF, Conrad PG, Downs RT. Crystal structure and Raman spectrum of hydroxyl-bästnasite-(Ce), $CeCO_3(OH)$. Am Mineral 2008;93(4):698–701.
[31] Maksimovi Z, Pant G. Hydroxyl-bastnaesite-(Nd), a new mineral from Montenegro, Yugoslavia. Mineral Mag 1985;49:717–20.
[32] Mariano AN, Mariano A. Rare earth mining and exploration in North America. Elements 2012;8:369–76.
[33] Ni Y, Post JE, Hughes JM. The crystal structure of parisite-(Ce), $Ce_2CaF_2(CO_3)_3$. Am Mineral 2000;85(1):251–8.
[34] Menezes F, Luiz AD, Chaves ML, Chukanov NV, Atencio D, Scholz R, Pekov I, da Costa GM, Morrison SM, Andrade MB, Freitas ET. Parisite-(La), ideally CaLa2(CO3)3F2, a new mineral from Novo Horizonte, Bahia, Brazil. Mineral Mag 2018;82(1):133–44.
[35] Menezes Filho LAD, Chaves MLSC, Chukanov NV, Atencio D, Scholz R, Pekov I, et al. Parisite-(La). Mineral Mag 2016;80:915–22.
[36] Jambor J, Burke E, Ercit T, Grice J. New mineral names. Am Mineral 1988;73:439–45.
[37] Zhang Peishan, Tao Kejie. Bayan Obo mineralogy. Beijing, China: Science Publisher; 1986; 208 [in Chinese with English summary].
[38] Zaitsev AN. Rhombohedral carbonates from carbonatites of the Khibina massif, Kola peninsula, Russia. Can Mineral 1996;34(2):453–68.
[39] Broom-Fendley S, Brady AE, Wall F, Gunn G, Dawes W. REE minerals at the Songwe Hill carbonatite, Malawi: HREE-enrichment in late-stage apatite. Ore Geol Rev 2017;81:23–41.
[40] Chakhmouradian AR, Wall F. Rare earth elements: minerals, mines, magnets (and more). Elements 2012;8:333–40.
[41] Förster HJ. Synchysite-(Y)–synchysite-(Ce) solid solutions from Markersbach, Erzgebirge, Germany: REE and Th mobility during high-T alteration of highly fractionated aluminous A-type granites. Mineral Petrol 2001;72:259–80.
[42] Maksimović Z, Pantó G. Minerals of the rare-earth elements in karstic bauxites: synchisite-(Nd), a new mineral from the Grebnik deposit. Proc. 4th International Congress for the study of bauxites, alumina, and aluminum, Athens; 1978. p. 540–53 [Abs. in Am. Mineral. 1979, 64, pp 658].
[43] Manfredi TR. A mineralização de parisita–(Ce) associada ao carbonatito Fazenda Varela. [Masters Thesis] Universidade Federal Do Rio Grande Do Sul Instituto de Geociencias; 2013.
[44] Al Ali S. Mineralogy and mineral processing to optimise recovery of synchysite-(Ce) and apatite from carbonatite at Songwe Hill, Malawi. [PhD Thesis] UK: University of Exeter; 2016.
[45] Mariano AN. Economic geology of rare earth elements. Rev Mineral Geochem 1989;21:309–37.
[46] Serdyuk SS, Lomayev VG, Kuzmin VI, Flett DS, Gudkova NV, Kuzmin DV, et al. The Chuktukon niobium-rare earth metals deposit: geology and investigation into the processing options of the ores. Miner Eng 2017;113:8–14.
[47] Jordens A, Sheridan RS, Rowson NA, Waters KE. Processing a rare earth mineral deposit using gravity and magnetic separation. Miner Eng 2014;62:9–18.
[48] Krishnamurthy N, Gupta CK. Extractive metallurgy of rare earths. CRC press; 2004.
[49] Keekan KK, Jalondhara JC, Abhilash. Extraction of Ce and Th from monazite using REE tolerant *Aspergillus niger*. Miner Process Extr Metall Rev 2017;38(5):312–20.
[50] Corbett MK, Eksteen JJ, Niu XZ, Croue JP, Watkin EL. Interactions of phosphate solubilising microorganisms with natural rare-earth phosphate minerals: a study utilizing Western Australian monazite. Bioprocess Biosyst Eng 2017;40(6):929–42.
[51] U.S. Geological Survey. Mineral commodity summaries 2016. U.S. Geological Survey; 2016; 202.
[52] Chelgani SC, Rudolph M, Leistner T, Gutzmer J, Peuker UA. A review of rare earth minerals flotation: monazite and xenotime. Int J Min Sci Technol 2015;25(6):877–83.
[53] Zhang Y, Anderson C. Surface chemistry and microflotation of xenotime and selected gangue minerals using octanohydroxamic acid as the collector. J Sustain Metall 2017;3(1):39–47.
[54] Zhang W, Honaker RQ, Groppo JG. Flotation of monazite in the presence of calcite part I: calcium ion effects on the adsorption of hydroxamic acid. Miner Eng 2017;100:40–8.
[55] Zhang W, Honaker R. A fundamental study of octanohydroxamic acid adsorption on monazite surfaces. Int J Miner Process 2017;164:26–36.
[56] Liu W, Wang X, Xu H, Miller JD. Lauryl phosphate adsorption in the flotation of Bastnaesite, $(Ce,La)FCO_3$. J Colloid Interface Sci 2017;490:825–33.
[57] Liu W, Wang X, Xu H, Miller JD. Physical chemistry considerations in the selective flotation of bastnaesite with lauryl phosphate. Miner Metall Process 2017;34(3):116–24.
[58] Fuerstenau DW. Trans AIME 1957;208:1365.
[59] Fuerstenau DW, Pradip. Zeta potentials in the flotation of oxide and silicate minerals. Adv Colloid Interface Sci 2005;114:9–26.
[60] Xu L, Peng T, Tian J, Lu Z, Hu Y, Sun W. Anisotropic surface physicochemical properties of spodumene and albite crystals: implications for flotation separation. Appl Surf Sci 2017;426:1005–102.
[61] Azizi D, Larachi F. Surface interactions and flotation behavior of calcite, dolomite and ankerite with alkyl hydroxamic acid bearing collector and sodium silicate. Colloids Surf, A 2018;537:126–38.
[62] Kosmulski M. IEP as a parameter characterizing the pH-dependent surface charging of materials other than metal oxides. Adv Colloid Interface Sci 2012;171:77–86.
[63] Delgado ÁV, González-Caballero F, Hunter RJ, Koopal LK, Lyklema J. Measurement and interpretation of electrokinetic phenomena. J Colloid Interface Sci 2007;309:194–224.
[64] Pavez O, Brandao PRG, Peres AES. Technical note — adsorption of oleate and octylhydroxamate on to rare-earths minerals. Miner Eng 1996;9:357–66.
[65] Cui H, Anderson CG. Fundamental studies on the surface chemistry of ancylite, calcite, and strontianite. J Sustain Metall 2017;3(1):48–61.
[66] Hunter RJ. Zeta potential in colloid science: principles and applications. Vo. 2, New York: Academic press; 2013.
[67] Greenwood R. Review of the measurement of zeta potentials in concentrated aqueous suspensions using electroacoustics. Adv Colloid Interface Sci 2003;106:55–81.
[68] Fuerstenau DW, Shibata J. On using electrokinetics to interpret the flotation and interfacial behavior of manganese dioxide. Int J Miner Process 1999;57:205–17.
[69] Smith RW, Steiner SD. Autoactivation in anionic flotation of bastnaesite. Solids Separation Processes, Vol. 4. Institute of Chemical Engineers Symposium Series; 1980. p. 1–12.
[70] Houot R, Cuif JP, Mottot Y, Samama JC. Recovery of rare earth minerals with emphasis on flotation process. International Conference on Rare Earth Minerals and Minerals for Electronic Uses. Hat Yai, TH: Prince Songkla University; 1991. p. 301–24.
[71] Jordens A, Marion C, Kuzmina O, Waters KE. Surface chemistry considerations in the flotation of bastnäsite. Miner Eng 2014;66:119–29.
[72] Azizi D, Sarvaramini A, Larachi F. Liquid-liquid mineral separation via ionic-liquid complexation of monazite and bastnäsite—an alternate route for rare-earth mineral beneficiation. Colloids Surf, A 2017;520:301–23.
[73] Kosmulski M. The pH dependent surface charging and points of zero charge. VI. Update. J Colloid Interface Sci 2014;426:209–12.
[74] Parks GA. The isoelectric points of solid oxides, solid hydroxides, and aqueous hydroxo complex systems. Chem Rev 1965;65:177–98.
[75] Pradip Li CC, Fuerstenau DW. Surface chemical characterization of bastnaesite through electrokinetics. KONA Powder Part J 2015;32:176–83.
[76] Azizi D, Larachi F, Latifi M. Ionic-liquid collectors for rare-earth minerals flotation — case of tetrabutylammonium bis(2-ethylhexyl)-phosphate for monazite and bastnäsite recovery. Colloids Surf, A 2016;506:74–86.
[77] Espiritu ERL, da Silva GR, Azizi D, Larachi F, Waters KE. The effect of dissolved mineral species on bastnäsite, monazite and dolomite flotation using benzohydroxamate collector. Colloids Surf, A 2017;539:319–34.
[78] Sarvaramini A, Azizi D, Larachi F. Hydroxamic acid interactions with solvated cerium hydroxides in the flotation of monazite and bastnäsite—experiments and DFT study. Appl Surf Sci 2016;387:986–95.
[79] Espiritu ERL, Da Silva GR, Waters KE. IMPC: XXVIII International Mineral Processing Congress Proceedings; 2016.
[80] Liu W, Wang X, Wang Z, Miller JD. Flotation chemistry features in bastnaesite flotation with potassium lauryl phosphate. Miner Eng 2016;85:17–22.
[81] Anderson CD. Improved understanding of rare earth surface chemistry and its application to froth flotation. [PhD Thesis] USA: Colorado School of Mines; 2015.
[82] Zhang X. Surface chemistry aspects of fluorite and bastnaesite flotation systems. [PhD Thesis] United States: The University of Utah; 2014.
[83] Zhou F, Wang LX, Xu ZH, Liu QX, Chi RA. Interaction of reactive oily bubble in flotation of bastnaesite. J Rare Earth 2014;32:772–8.
[84] Herrera-Urbina R, Pradip, Fuerstenau DW. Electrophoretic mobility and computations of solid-aqueous solution equilibria for the bastnaesite-H_2O system. Miner Metall Process 2013;30:18–23.
[85] Zhang X, Du H, Wang X, Miller JD. Surface chemistry considerations in the flotation of rare-earth and other semisoluble salt minerals. Miner Metall Process 2013;30:24–37.
[86] Kim JA, Dodbiba G, Fujita T, Fujii N. Characteristics analysis of a bastnaesite rare earth mineral for recovery of cerium. IMPC XXV International Mineral Processing Congress, Brisbane, ALD, Australia; 2010. p. 2927–32.
[87] Ren J, Song S, Lopez-Valdivieso A. Selective flotation of bastnaesite from monazite in rare earth concentrates using potassium alum as depressant. Int J Miner Process 2000;59:237–45.

[88] Ren J, Lu S, Song S, Niu J. A new collector for rare earth mineral flotation. Miner Eng 1997;10:1395–404.
[89] Smith RW, Shonnard D. Electrokinetic study of the role of modifying agents in flotation of salt-type minerals. AIChE J 1986;32:865–8.
[90] Luo J, Chen X. Research into the recovery of high-grade rare-earth concentrate from Baotou Complex iron ores, China. Miner Process Ext Metall 1984:663–75.
[91] Li C. Solubility and electrokinetic behavior of synthetic bastnaesite. [Masters Thesis] Berkeley, USA: University of California; 1982.
[92] Pradip. The surface properties and flotation of rare-earth minerals. [Ph.D. Thesis] Berkeley, CA, USA: University of California; 1981; 222.
[93] Lafuente B, Downs RT, Yang H, Stone N. The power of databases: the RRUFF project. In: Gruyter De, editor. Highlights in mineralogical crystallography; 2016. p. 1–29 [DOI:].
[94] Bhushan SK. Geology of the Kamthai rare earth deposit. J Geol Soc India 2015;85(5):537–46.
[95] Tucker RD, Belkin HE, Schulz KJ, Peters SG, Horton F, Buttleman K, et al. A major light rare-earth element (LREE) resource in the Khanneshin carbonatite complex, southern Afghanistan. Econ Geol 2012;107(2):197–208.
[96] Yang X, Satur JV, Sanematsu K, Laukkanen J, Saastamoinen T. Beneficiation studies of a complex REE ore. Miner Eng 2015;71:55–64.
[97] Satur JV, Calabia BP, Hoshino M, Morita S, Seo Y, Kon Y, et al. Flotation of rare earth minerals from silicate–hematite ore using tall oil fatty acid collector. Miner Eng 2016;89:52–62.
[98] Metz MC, Brookins DG, Rosenberg PE, Zartman RE. Geology and geochemistry of the Snowbird deposit, Mineral County, Montana. Econ Geol 1985;80(2):394–409.
[99] Samson IM, Wood SA, Finucane K. Fluid inclusion characteristics and genesis of the fluorite-parisite mineralization in the Snowbird Deposit, Montana. Econ Geol 2004;99(8):1727–44.
[100] Metz MC. The geology of the Snowbird deposit, Mineral Co., Montana. [MSc Thesis] Washington State University; 1971.
[101] Miyawaki R, Yokoyama, Husdal TA. Bastnäsite-(Nd), a new Nd-dominant member of the bastnäsite group from the Stetind pegmatite, Tysfjord, Nordland, Norway. Eur J Mineral 2013;25(2):187–91.
[102] Pavese A, Catti M, Parker SC, Wall A. Modelling of the thermal dependence of structural and elastic properties of calcite, $CaCO_3$. Phys Chem Miner 1996;23(2):89–93.
[103] Hunt JA, Berry RF. Geological contributions to geometallurgy: a review. Geosci Can 2017;44(3):103–18.
[104] Fuerstenau DW, Pradip, Herrera-Urbina R. The surface chemistry of bastnaesite, barite and calcite in aqueous carbonate solutions. Colloids Surf 1992;68:95–102.
[105] Al Mahrouqi D, Vinogradov J, Jackson MD. Zeta potential of artificial and natural calcite in aqueous solution. Adv Colloid Interface Sci 2016;240:60–76.
[106] Voigt M, Rodriguez-Blanco JD, Vallina B, Benning LG, Oelkers EH. An experimental study of hydroxylbastnasite solubility in aqueous solutions at 25 °C. Chem Geol 2016;430:70–7.
[107] Croll R, Swinden S, Hall M, Brown C, Beer G, Scheepers J, et al. Mkango Resources Limited, Songwe REE Project, Malawi: NI 43-101 pre-feasibility report. Technical report. MSA Group (Pty) Ltd; 2014.
[108] Jordens A, Marion C, Grammatikopoulos T, Hart B, Waters KE. Beneficiation of the Nechalacho rare earth deposit: flotation response using benzohydroxamic acid. Miner Eng 2016;99:158–69.
[109] Yu B, Aghamirian M. REO mineral separation from silicates and carbonate gangue minerals. Can Metall Quart 2015;54:377–87.
[110] Owens Camilla, University of Exeter. Zeta potential measurements of the fluorcarbonate mineral parisite. British Geological Survey 2018. https://doi.org/10.5285/3c145498-37b5-4935-b5fe-baae2db64054.